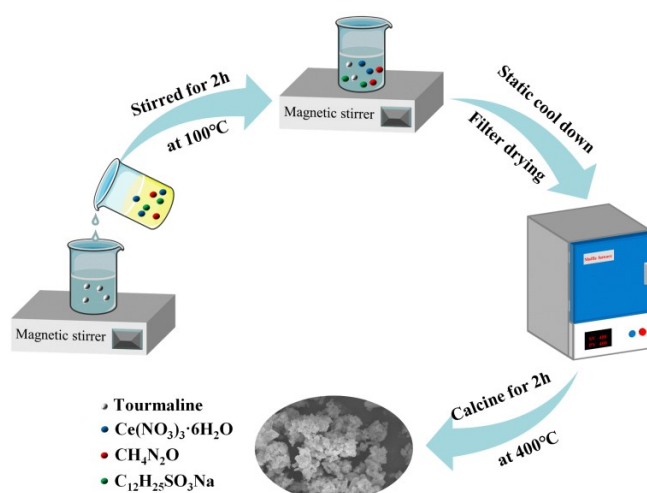


CeO₂ stabilized by tourmaline as a novel inorganic filler to simultaneously increase the conductivity and durability of proton exchange membranes

contents



Scheme S1. The synthetic process of Tourmaline-CeO₂.

Table S1. IEC, hydration number at 80°C of membranes.

Samples	IEC (mmol/g)	H ₈₀ (n(H ₂ O)/n(SO ₃ ⁻))
Pristine PFSA	1.050	13.889
PFSA/TM-CeO ₂ (0.5wt%)	1.037	15.107
PFSA/TM-CeO ₂ (1wt%)	1.021	17.401
PFSA/TM-CeO ₂ (1.5wt%)	1.029	18.492
PFSA/TM-CeO ₂ (2wt%)	0.984	20.562

Table S2. Comparison of proton conductivity and fuel cell performance for pristine
 PFSA and PFSA/TM-CeO₂ (1wt%) composite membranes.

Samples	Proton conductivity (mS cm ⁻¹)	Power density (mW cm ⁻²)	OCV degradation rates (mV/h)
Pristine PFSA	143.91	906	2.18
PFSA/TM-CeO ₂ (1wt%)	155.51	1006	0.29

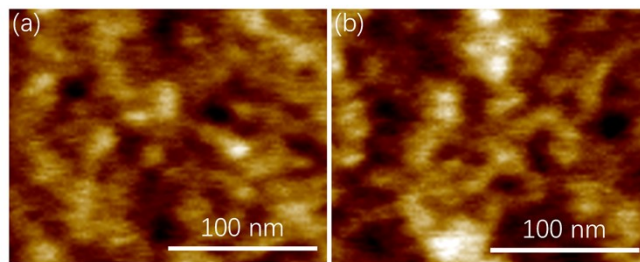


Fig. S1. AFM images of (a) pristine PFSA and (b) PFSA/TM-CeO₂ (1wt%).

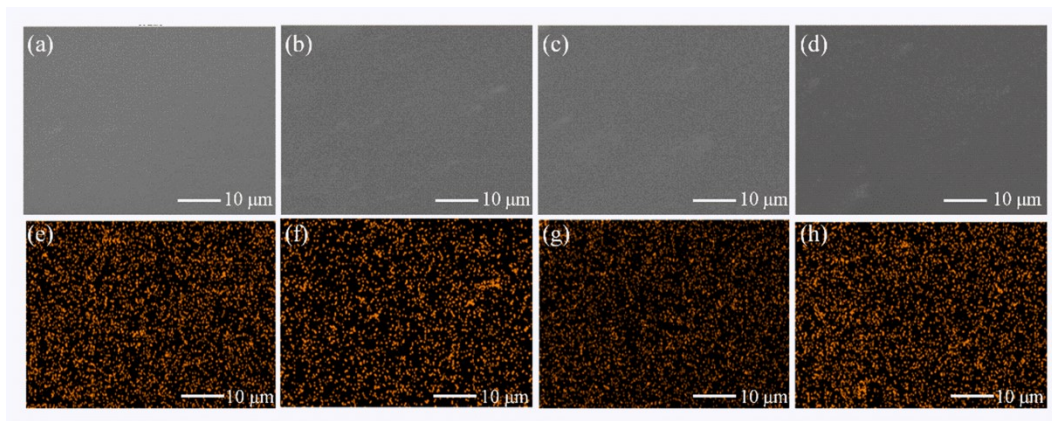


Fig. S2. Surface SEM-EDS mappings of Ce element distribution for the various composite membranes. (a, e) PFSA/TM-CeO₂ (0.5wt%); (b, f) PFSA/TM-CeO₂ (1wt%); (c, g) PFSA/TM-CeO₂ (1.5wt%); (d, h) PFSA/TM-CeO₂ (2wt%).

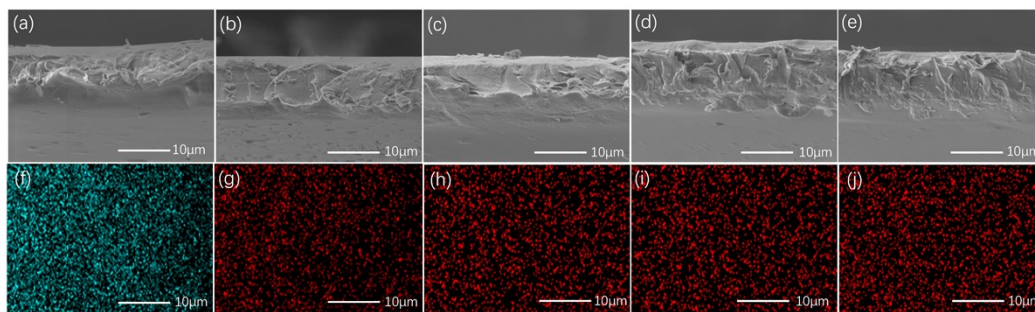


Fig. S3. Cross SEM-EDS mappings of O or Ce element distribution for the various composite membranes. (a, f) pristine PFSA; (b, g) PFSA/TM-CeO₂ (0.5wt%); (c, h) PFSA/TM-CeO₂ (1wt%); (d, i) PFSA/TM-CeO₂ (1.5wt%); (e, j) PFSA/TM-CeO₂ (2wt%).

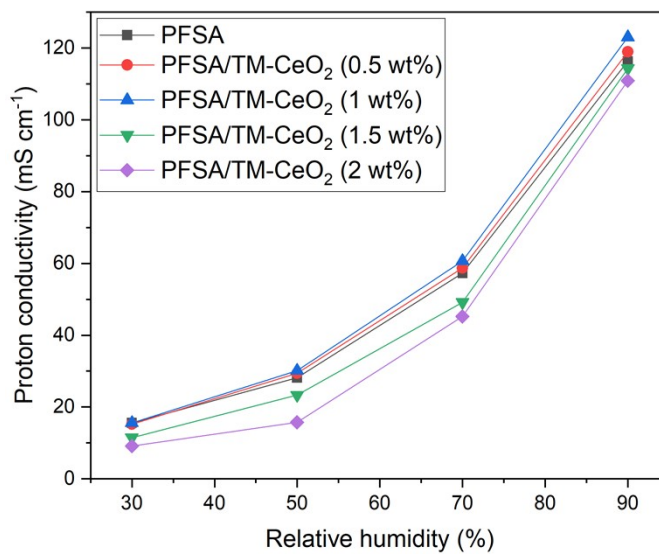


Fig. S4. HFR of Proton conductivity of pristine PFSA and various PFSA/TM-CeO₂ (X wt%) composite membranes at different relative humidity under 80°C.

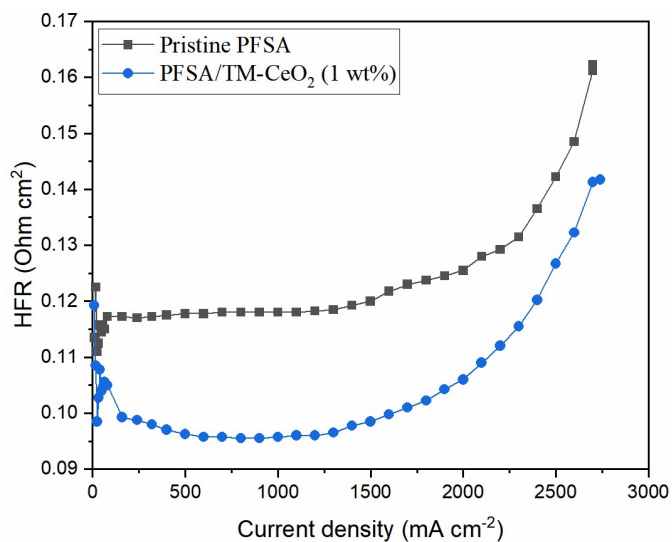


Fig. S5. HFR of MEAs corresponding to pristine PFSA, PFSA/TM-CeO₂ (1wt%) composite membranes.

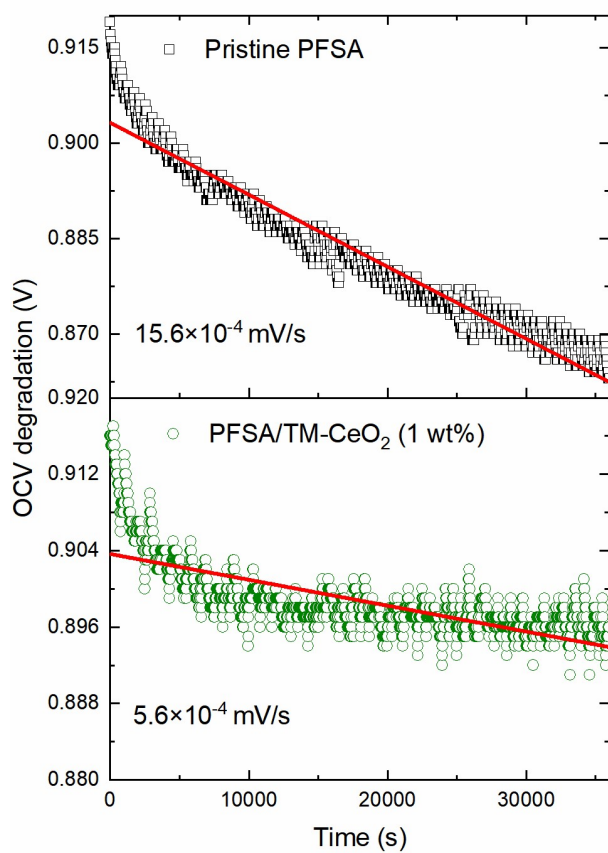


Fig. S6. Durability curves of pristine PFSA and PFSA/TM-CeO₂ (1wt%) membranes at 90°C and 30% RH.

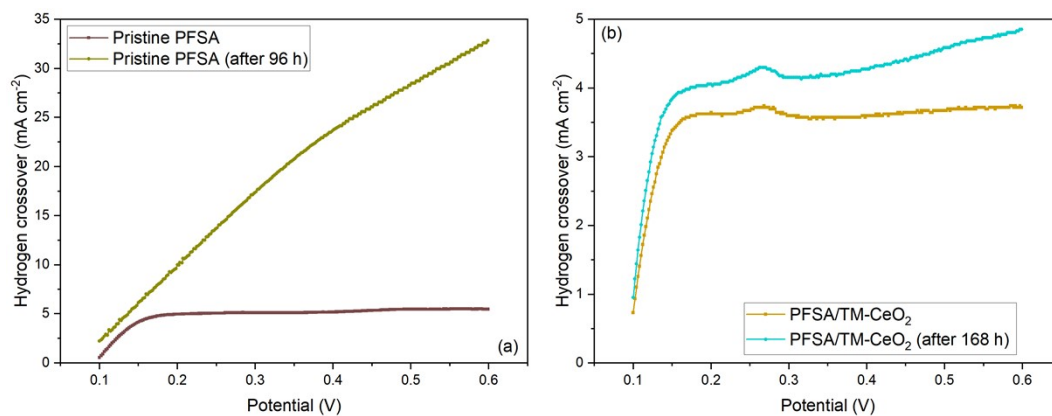


Fig. S7. Hydrogen crossover of the pristine PFSA, PFSA/TM-CeO₂ (1wt%) composite membranes before and after OCV.